Chapter in **Advancing Astrophysics with the SKA – II**

Exploring the physics of ram pressure stripping with radio continuum observations in the SKA era

Alessandro Ignesti [1], Ian D. Roberts [2,3] Henrik W. Edler [4,5] Myriam Gitti [6,7] Reinout J. van Weeren [8] Paolo Serra [9] and Pavel Jachym [10]

[1] *INAF - Astronomical Observatory of Padova, vicolo dell'Osservatorio 5, 35122 Padova, Italy*

[2] *Waterloo Centre for Astrophysics, University of Waterloo, 200 University Avenue West, Waterloo, ON, N2L 3G1, Canada*

[3] *Department of Physics & Astronomy, University of Waterloo, 200 University Avenue West, Waterloo, ON, N2L 3G1, Canada*

[4] *ASTRON, Netherlands Institute for Radio Astronomy, Oude Hoogeveensedijk 4, 7991 PD Dwingeloo, The Netherlands*

[5] *Hamburger Sternwarte, University of Hamburg, Gojenbergsweg 112, D-21029, Hamburg, Germany*

[6] *Dipartimento di Fisica e Astronomia (DIFA), Università di Bologna, via Gobetti 93/2, 40129 Bologna, Italy*

[7] *INAF - Istituto di Radioastronomia, via P. Gobetti 101, Bologna, Italy*

[8] *Leiden Observatory, Leiden University, PO Box 9513, 2300 RA Leiden, The Netherlands*

[9] *INAF,Osservatorio Astronomico di Cagliari, Via della Scienza 5, Selargius, 09047, CA, Italy*

[10] *Academy of Sciences, Boční II 1401, 141 00, Prague, Czech Republic*

E-mail: alessandro.ignesti@inaf.it

Satellite galaxies in clusters are significantly more likely to be red and passive than similar mass galaxies in the field. This fact is known as the environmental quenching of galaxy star formation, which is believed to be driven by ram pressure stripping (RPS). The large velocity differences between the infalling galaxies and the intracluster medium (ICM) result in a strong ram pressure on their interstellar medium (ISM), which can strip it from the stellar disk. The stripped ISM can be studied at various wavelengths, including the radio band, thanks to the synchrotron emission produced by the magnetic fields and relativistic electrons embedded in them. This emission is typically steep-spectrum and thus best observed at low frequencies. Thus, continuum studies of the RPS effect are currently mostly carried out with LOFAR, limiting them to the northern hemisphere. SKA-Low will permit us to extend them to the southern sky, where they will synergize with the southern observatories and the upcoming ELT. Lastly, the sub-arcsecond resolution provided by SKA-Mid will facilitate the exploration of the polarization and filamentary structure of RPS radio tails and allow us to detect them up to $z \simeq 0.5$, advancing our understanding of the impact of RPS on satellite galaxies in clusters and groups.

© The Authors

1 Environmentally-driven galaxy evolution

The balance between the gas inflow and removal drives the baryon cycles in galaxies, and thus their evolution. Whereas the inflows sustain star formation and allow galaxies to grow in mass, gas removal can lead to star formation quenching. Galaxies can lose their gas via internal or external processes. The latter, generally known as environmental effects, are crucial in shaping galaxy properties in clusters and groups (Dressler, 1980; Vulcani et al., 2022; Boselli et al., 2022). They can be divided into two main categories, those driven by gravitational forces between galaxies, such as mergers and tidal interaction (Barnes and Hernquist, 1992) or harassment due to fast encounters (Moore et al., 1996), and those resulting from the hydrodynamical interaction between the galaxies and the environmental plasma, either the intracluster medium (ICM) or the intragroup medium (IGrM). This category includes thermal evaporation (McKee and Cowie, 1977), viscous stripping (Nulsen, 1986), and ram pressure stripping (RPS, Gunn and III, 1972). The latter is the external pressure exerted by the environmental plasma on a moving body, typically expressed as $P_{\rm ram} = \rho V^2$ where ρ is the medium density and V is the object velocity. In the most extreme cases, ram pressure can overcome the stellar disk binding force and strip the circumgalactic and interstellar medium (ISM) components from the galaxy (Gunn and III, 1972). The gas loss induced by RPS can effectively quench the star formation in the stellar disk (Boselli et al., 2022, for a review), thus making it an important quenching pathway for satellite galaxies (e.g., Vollmer et al., 2001; Tonnesen et al., 2007; Vulcani et al., 2020; Watts et al., 2023). Although RPS is expected to be the strongest during the galaxies' first infall, especially for galaxies following the most radial orbits (Biviano et al., 2024), optical studies revealed that almost all galaxies in clusters undergo an RPS event within their lifetime (Vulcani et al., 2022). Moreover, due to the difference in the average environmental plasma density and satellite velocities, RPS is expected to dominate the galaxy evolution in clusters, where due to the large masses ($> 10^{14}$ $M_\odot$) galaxies have a typical velocity dispersions of several hundreds to thousand of kilometers per second and the medium particle density is of the order of $10^{-4} - 10^{-3}$ cm^{-3}, but thought to be less relevant in galaxy groups, lower mass systems ($< 10^{14}$ $M_\odot$) where gravitational interactions are more frequent due to the generally smaller velocity dispersion. The ram pressure action is not limited to displacing the ISM outside of the disk. The impact of ram pressure can result in many effects, including compression of gas along the leading edge of the disk (e.g., Rasmussen et al., 2006; Poggianti et al., 2019; Roberts et al., 2022a), disturbed galaxy morphologies, trailing tails of

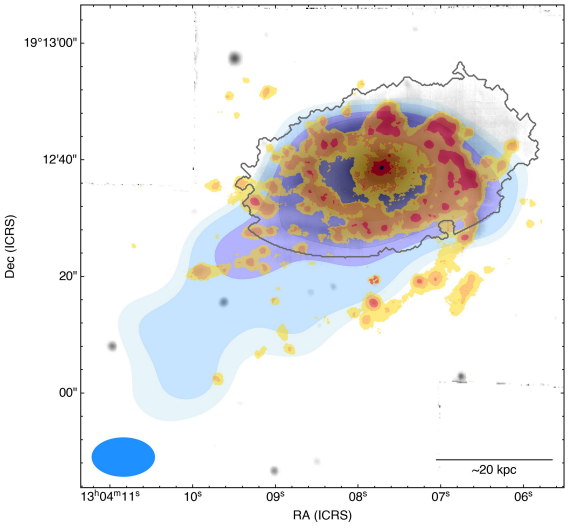

Figure 1: Composite optical-radio image of the RPS galaxy JW39 from Ignesti et al. (2022a). Here are reported the stellar continuum (greyscale), stellar disk (silver contour), Hα emission (yellow-to-red contours) and radio continuum emission at 144 MHz (blue-filled contours).

stripped gas (e.g., Kenney et al., 2004; van Gorkom, 2004; Fumagalli et al., 2014; Poggianti et al., 2017b), and condensation of star-forming knots in the tails (Kenney et al., 2014; Poggianti et al., 2019). It can also temporarily enhance the global star formation (e.g., Poggianti et al., 2016; Vulcani et al., 2018; Roberts and Parker, 2020) and trigger the activity of the central nuclei (e.g., Poggianti et al., 2017a; Peluso et al., 2022). Indeed it has been observed that it can affect the microphysics of the ISM on small scales, for example by stimulating the conversion from atomic to molecular hydrogen (Moretti et al., 2020), enhancing the diffusivity of cosmic rays (Farber et al., 2022; Ignesti et al., 2022a), or by inducing mixing between the ISM and ICM (Sun et al., 2021; Franchetto et al., 2021). The most extreme examples of galaxies undergoing strong RPS are the so-called jellyfish galaxies (Fumagalli et al., 2014; Smith et al., 2010; Ebeling et al., 2014; Poggianti et al., 2017b). In the optical/UV band, these objects show extraplanar, unilateral debris extending beyond their stellar disks, and striking tails of ionised gas hosting star-forming regions (Figure 1). Jellyfish galaxies mostly reside in galaxy clusters and are a transitional phase between infalling star-forming spirals and quenched cluster galaxies; for this reason, they provide a unique opportunity to understand the impact of gas-removal processes on galaxy evolution.

2 Exploring the physics of ram pressure stripping with radio continuum observations

A number of ram pressure stripped galaxies have been observed to show tails of radio continuum emission extending for tens of kiloparsecs from their stellar disk (e.g., Gavazzi and Jaffe, 1987; Murphy et al., 2009; Vollmer et al., 2013; Chen et al., 2020; Müller et al., 2021; Roberts et al., 2021b, 2022b; Ignesti et al., 2022a). These radio tails typically develop steep-spectrum emission ($\alpha < -0.9$ at GHz frequencies) within few tens of kiloparsecs from the stellar disk (e.g., Vollmer et al., 2004; Chen et al., 2020; Ignesti et al., 2022b; Müller et al., 2021; Lal et al., 2022; Venturi et al., 2022; Roberts et al., 2024b). Therefore, they are best observed below GHz frequencies, and for this reason, the LOw Frequency ARray (LOFAR, van Haarlem et al., 2013) has been revolutionary for the study of RPS in clusters and groups. Specifically, the LOFAR Two-metre Sky Survey (LoTSS, Shimwell et al., 2017, 2019; Shimwell et al., 2022) has provided high-resolution (6“) and highly sensitive ($\sim$ 100 μJy beam^{-1}) images of the Northern sky at 120-168 MHz, revealing that at low frequencies, the stripped tails can extend for up to 100 kpc in the galaxies' wakes, making them easily detectable in the radio sky (Figure 2). Thanks to LOFAR, over one hundred new RPS galaxies have been discovered in the northern sky with an occurrence rate varying from 10 to 20% (Roberts et al., 2021b). This indicates that RPS is not an isolated occurrence but rather a common phase experienced by the majority of cluster galaxies. With this relatively large sample size, it is now possible to conduct statistical studies of the RPS radio continuum tail development in clusters (see Smith et al., 2022, for a recent example).

RPS deeply affects the galaxies' nonthermal radio emission, from the microphysics regulating the ISM up to the overall morphology. In general, radio continuum emission in spiral galaxies is composed of the thermal emission from the $\sim 10^4$ K plasma in the HII regions produced via thermal bremsstrahlung, and the non-thermal synchrotron emission of the relativistic cosmic rays electrons (CRe), which are accelerated by supernovae shocks reaching energies of a few GeV (e.g.

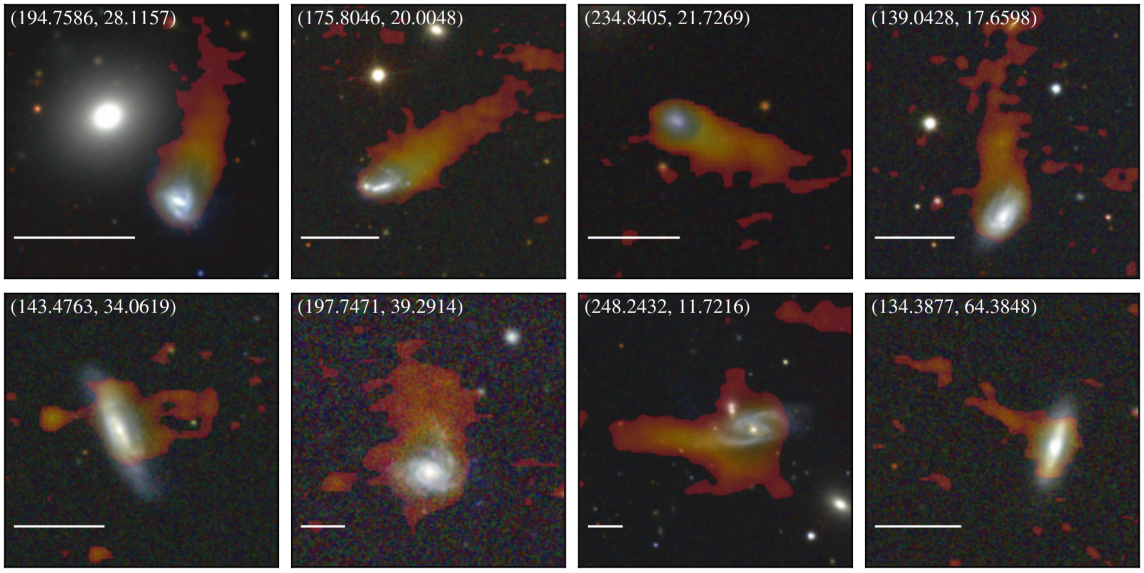

Figure 2: Composite optical (CFHT, RGB) and radio (LOFAR, 144 MHz) images of eight LoTSS jellyfish galaxies from Roberts et al. (2021a,b) at $z < 0.04$. The galaxy celestial coordinates are reported in the top-left corner, and the white scalebar corresponds to a size of 20 kpc at the hosting cluster redshift.

Condon, 1992, for a review). Given the connection between star-formation and CRe and the fact that galaxies are generally optically-thin to radio wavelengths, the continuum radio emission is a reliable proxy to evaluate their star formation rate (SFR) (e.g., Kennicutt and Evans, 2012). At GeV energies, CRe energy losses are dominated by synchrotron emission in the galactic magnetic fields with typical values of 10-30 μG (e.g., Beck and Krause, 2005, and references therein), which results in nonthermal radio emission in the 100 MHz-10 GHz band, and Inverse Compton scattering with the galactic and stellar radiation field (e.g., Pacholczyk, 1970; Longair, 2011). Star-forming galaxies in clusters usually show a large scatter in the radio luminosity-SFR relation with respect to isolated galaxies (Chen et al., 2020), whereas RPS galaxies are typically in excess of radio luminosity with respect to their ongoing star formation rate. The excess can either be real, induced by the amplification of the ISM magnetic field by turbulence and compression, or apparent, resulting from a mismatch between the declining star formation rate and the CRe radiative time-scale (Ignesti et al., 2022a; Edler et al., 2024). Finally, by comparing the resolved spatial correlation between Hα emission, which traces the ionized gas and, hence, the star-forming regions, and low-frequency radio continuum, which maps the nonthermal ISM, it has been observed that that the typical CRe transport scale in these extreme galaxies is 5-10 kpc, which is larger than the average values of 1-5 kpc measured in nearby, isolated systems (Ignesti et al., 2022a; Edler et al., 2024).

RPS is also responsible for the formation of the radio continuum tails, produced by the CRe accelerated in the stellar disk (Condon, 1992). Multifrequency studies observed that spectral index steepens with radial distance along these tails (e.g., Vollmer et al., 2004; Chen et al., 2020; Müller et al., 2021; Ignesti et al., 2022b; Roberts et al., 2022b; Venturi et al., 2022), suggesting the following scenario. After the injection, the relativistic electrons are stripped, together with the ISM, from the disk by the ram pressure. The CRe cool down by emitting radio waves via synchrotron radiation

in the stripped ISM magnetic field and Inverse Comption losses with the CMB until the stripped clouds evaporate in the ICM. This way, RPS contributes to the accumulation of low-energy CRe and magnetic fields in the ICM which are available as seed-electrons for re-acceleration by ICM turbulence and shocks (de Gasperin et al., 2026). The stripped tail magnetic field can be further amplified by the ICM magnetic draping (Dursi and Pfrommer, 2008; Pfrommer and Dursi, 2010; Ruszkowski et al., 2014; Müller et al., 2021). In this framework, the radio tail length would be mainly driven by two factors, the CRe cooling time (Pacholczyk, 1970), and the radio plasma bulk velocity along the stripping direction. The synchrotron emission frequency, ν, of a single CRe depends on its energy, E, and the magnetic field intensity, B, as $\nu \propto E^2 B$. Therefore, under the assumption that the relativistic electrons move in a uniform velocity bulk motion in a uniform magnetic field, then the tail scale length D would decrease with the observed frequency as $D \propto \nu^{-1/2}$ (Ignesti et al., 2022b).

This basic relation entails that to grasp the full tail extent is necessary to observe them at low frequencies. An interesting implication of this framework is that the flux density gradient along the tail, for a given magnetic field intensity, depends on the stripped ISM velocity. Therefore, by fitting the spectral curvature across wideband data, it is possible to constrain the stripped ISM velocity along the plane of the sky and, correspondingly, the galaxy velocity with respect to the ICM (Ignesti et al., 2023; Roberts et al., 2024b,a), which makes radio continuum observations a valuable tool to constrain the galaxy dynamics in the cluster. Finally, LOFAR has proven that radio continuum tails are observed also in galaxies without clear evidence of ongoing RPS in the optical band, which instead appear only in the most extreme cases. Moreover, the large primary beam at low frequency allows us to map the entire cluster volume, which further contributes in making radio-selected samples less biased than more targeted spectroscopic observations. Therefore, radio-selected RPS galaxies can be adopted to build less biased samples for follow-up optical studies.

A current open question regards the properties of the magnetic field and its role in regulating the ISM-ICM mixing. The stripped ISM, with typical temperature of 10^{2-5} K, (Spitzer, 1978) can interact with the ICM, which is a weakly magnetized plasma characterized by a density of 10^{-4} – 10^{-3} particles cm^{-3}, a temperature of 10^{7-8} K (Sarazin, 1988), and μG-level magnetic fields (Govoni and Feretti, 2004). The large temperature and velocity differences between the two phases imply short evaporation timescales for the stripped ISM ($\sim 10^{7-8}$ yr, Klein et al., 1994) due to a combination of hydrodynamical instabilities and thermal conduction. As the typical stripping timescales are an order of magnitude larger ($\sim 10^{8-9}$ yr, Smith et al., 2022; Rohr et al., 2023), the expectation is that the stripped ISM will completely evaporate in the ICM while being stripped. Yet, in jellyfish galaxies, we observe trails of stripped ISM extending for tens of kpc and hosting active star-forming regions. This result proves the existence of a mechanism that can stabilize the stripped ISM, thus extending its survival outside of the stellar disk and permitting it to cool down and form new stars. A possible explanation for the ISM cooling in the hostile ICM conditions is the presence of ordered magnetic fields at the hot-cold plasmas interface, which can dampen the thermal conduction between the hot and cold phases and stabilize against hydrodynamical instabilities (McCourt et al., 2015; Sparre et al., 2020, 2024; Sparre et al., 2024), as well as reducing the gas mass loss (Rintoul et al., 2025).

The presence of magnetic fields in the stripped material is naturally expected due to both internal and external factors. On the one hand, the stripped material is expected to be magnetized because it contains the ISM magnetic field bound to the thermal gas being removed by the ram pressure (Vollmer et al., 2004; Ignesti et al., 2023; Vollmer et al., 2024). In this scenario, due to the turbulent, small-scale motions in the stripped material (Li et al., 2023; Ignesti et al., 2024; Choi et al., 2026) the stripped tail is expected to show a low degree of polarized synchrotron emission, as consequence of the magnetic field disordered structure and the strong Faraday depolarization resulting from the thermal plasma mixed with the nonthermal components.

On the other hand, the weak magnetic field permeating the ICM can accumulate around the infalling galaxy via the so-called magnetic draping (Dursi and Pfrommer, 2008; Pfrommer and Dursi, 2010), which would naturally provide a way for jellyfish galaxies to surround themselves with large-scale magnetic fields accreted from the environment. Numerical simulations (Dursi and Pfrommer, 2008) indicate that a prerequisite for the formation of the large-scale, ordered magnetic drape is that the galaxy's velocity must exceed the local Alfvén speed $V_A = B/\sqrt{4\pi\rho}$, where B is the magnetic field and ρ is the ion mass density, to bend the external magnetic field on its surface. This condition is virtually always satisfied in galaxy clusters, where the typical ICM Alfvén speed is of the order of several tens of km s^{-1} and the cluster velocity dispersion is typically of the order of several hundreds of km s^{-1} (Girardi et al., 1993). Furthermore, in the case of supersonic motion, the ICM magnetic field can be significantly amplified at the curved bow-shock propagating into an inhomogeneous ICM, which adiabatically enhances the ICM magnetic field via shock compression and injects turbulence that could further amplify the magnetic field via a small-scale dynamo. In fact, for galaxies moving supersonically in the ICM, numerical simulations predict the formation of an ordered magnetic drape extending for tens of kpc in the galaxy wake (Sparre et al., 2020, 2024). This mechanism would be the one responsible for the formation of an ordered field "shielding" the stripped material. In this scenario, the galaxy is also expected to show a high degree of polarized emission thanks to the magnetic field being ordered on large scales and the fact that it would be less affected by the Faraday depolarization induced by the stripped material. As in galaxy clusters, the speed of sound is comparable to the cluster velocity dispersion, supersonic draping is expected to be at work for jellyfish galaxies, which typically are the fastest cluster galaxies (Jaffé et al., 2018), providing a potential explanation for the origin of the long star-forming tails (Ignesti et al., 2026). On the contrary, due to the mostly unknown properties of galaxy groups' magnetic fields, the role of magnetic draping in less massive halos is still unexplored. However, detecting polarized emission from the RPS tails is challenging and it requires balancing two competing factors: the surrounding ICM Faraday rotation, which depolarizes the emission, especially at low frequencies, and the intrinsic steep-spectrum nature of the radio continuum tails with a scale length decreasing with the CRe energy, which prevents their detection at high frequencies. Therefore, we currently lack a census of polarized properties for RPS galaxies that could help us test the model.

3 Studying the physics of ram pressure stripping in the SKA era

The Square Kilometre Array will be crucial to push forward the current studies on RPS. Although providing exact estimates on its impact is not trivial, due to the transitory nature of the RPS phase

for cluster galaxies, where the duration depends on the infalling orbit and the galaxy mass, and the intrinsic dependence on projection effects, which can hide the RPS features, in the following the provide a framework to evaluate the potential impact of SKA observations. The combination of the intrinsic radio tail properties and the ICM depolarization makes that the full radio tail extension can be observed mainly below 200 MHz, whereas its polarized emission becomes visible above GHz frequencies. This behavior is exemplified in Figure 3 (top panel), where we compare the simplified radio tail spectral contraction (Ignesti et al., 2022b) with the corresponding ICM depolarization for typical ICM conditions (RM$>$ 10 rad m^{-2}) at increased observed frequency. From this comparison, it emerges that, for moderate ICM depolarization, the radio band around 1 GHz could have the optimal conditions to observe both a significant tail extent with, potentially, a non-negligible polarization fraction. Moreover, due to the high angular resolution, SKA-Mid Band 1 observations will be able to resolve the magnetic field structure on sub-kpc scale for $z < 0.05$, thus future observations could be able to detect the small-scale polarized emission associated with the stripped ISM magnetic field and, possibly, disentangle it from the large-scale polarized emission associated with the external ICM drape. When taking into consideration the frequency bands that will be covered by SKA, it becomes clear that SKA-Low and, to a lower extent, SKA-Mid Band 1 will be able to observe most of their the radio tail's full extent, hence facilitating locating RPS candidates in wide-field observations. Moreover, SKA-Low will operate in the southern sky with a greater sensitivity and bandwidth than LOFAR, with a resolution comparable to the current wide-area surveys, greatly increasing the number of galaxies with evidence for ongoing RPS. Having access to a large sample of RPS galaxies will permit us, for the first time, to assess the effects of the cluster/group dynamics on RPS galaxy fraction (Lourenço et al., 2023). Finally, opening the southern sky will be important for multi-wavelength studies as well because it will permit synergies with the Southern Observatories such as VLT, ALMA and ELT, which are characterized by high angular resolution but small field of view, hence they are less suited for wide-field surveys. Combining these instruments will permit us to carry out multi-wavelength, high-resolution follow-up observations for new RPS candidates found by SKA-Low to assess how the different ISM components, nonthermal, molecular and ionized, evolve under the effect of RPS. We also note that an important feature of studying RPS in dense environments is that they greatly synergize with dedicated galaxy clusters and groups studies, such as the search for diffuse radio continuum emission on Mpc scales, or polarimetric surveys that will map the clusters' magnetic fields, representing an excellent ancillary case for future, wide-field observations which can lead to serendipitous detection of new RPS candidates.

Concerning the study of polarized emission, with the exciting prospect of finally exploring the elusive extraplanar magnetic fields, SKA-Mid Band 2 will fall in the 'sweet spot' at 1.4 GHz in which it will be possible to detect a significant fraction of both the radio tail extent and its intrinsic polarized emission. Therefore, SKA-Mid will be able to explore two crucial open questions, map the magnetic field of RPS galaxies, potentially down to sub-kpc scale thanks to the sub-arcsecond resolution achievable in AA4 configuration (Loi et al., 2026), and investigate the interplay between neutral and relativistic ISM components under ram pressure. The first will address our primary open questions and, regarding the latter, observation at 1.4 GHz will simultaneously trace the synchrotron nonthermal radio emission and the neutral hydrogen 21-cm radiation, which is a crucial tracer for

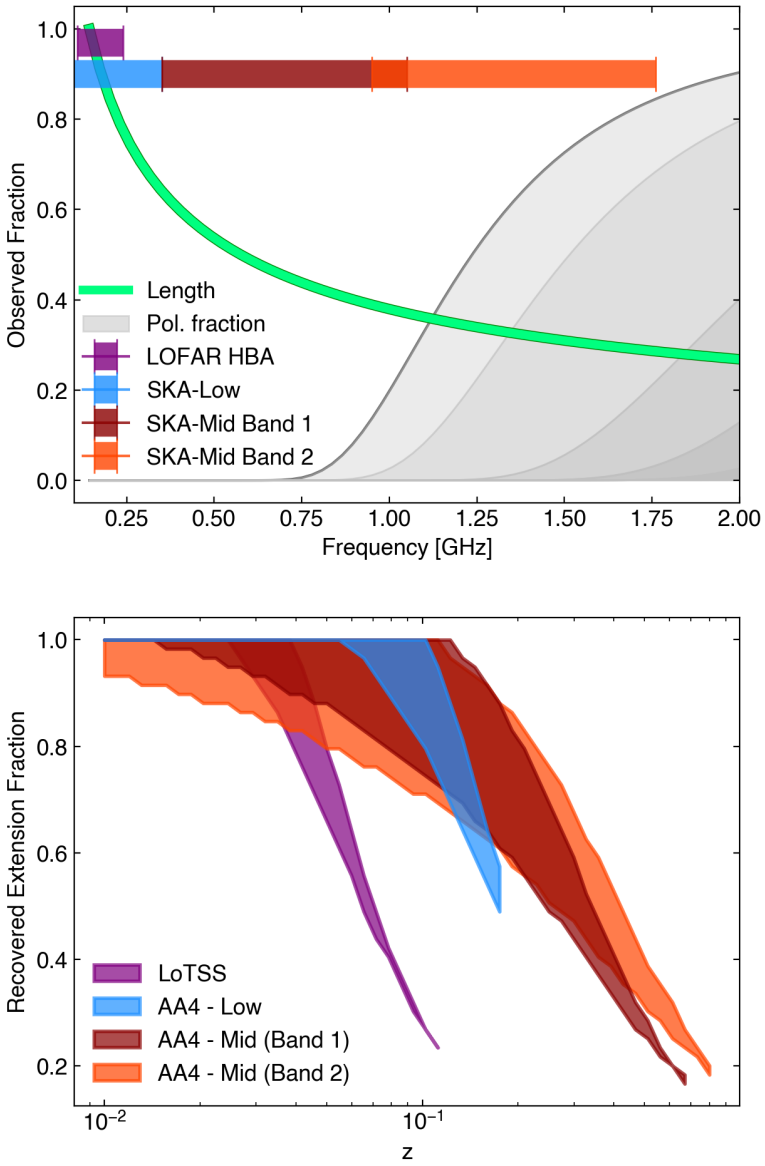

Figure 3: *Top:* Reference evolution of radio tail scale length (green) and polarization fraction (silver, darker shades correspond to increasing ICM rotation measure levels of -10, -15, -30, -45, and -60 rad m^{-2}) with the observed frequency. The horizontal bars indicate the frequency band observed by LOFAR HBA (purple), SKA-Low (blue), SKA-Mid band 1 (red) and band 2 (orange). *Bottom:* Recovered RPS radio tail observed fraction by LOFAR LoTSS and the different SKA configurations at increasing redshift. For each configuration, we report here the angular resolution, θ, and the expected RMS, σ: LoTSS $\theta = 6$ arcseconds, $\sigma = 100$ μJy beam^{-1}; AA4-Low $\theta = 9$ arcseconds, $\sigma = 12$ μJy beam^{-1}; AA4-MID (B1) $\theta = 1$ arcseconds, $\sigma = 2$ μJy beam^{-1}; AA4-MID (B2) $\theta = 0.8$ arcseconds, $\sigma = 1$ μJy beam^{-1}

environmental processing (for a detailed discussion, we refer to Ramatsoku et al., 2026).

Combining SKA Low and Mid observations will allow us to routinely measure the spectral properties of RPS tails across a large bandwidth from 200 to 2000 MHz. This will allow us to constrain the

dynamics of the infalling galaxies and the time scales of the RPS for large samples. For reference, an exposure time of 1 hr with SKA-Low and SKA-Mid band 2 in AA4 configuration taken in the full corresponding bandwidths[1] will result in continuum noise levels at 200 and 1300 MHz of, respectively, 11.1 and 2.7 μJy beam^{-1} for similar angular resolution of 9 arcseconds with `robust=0`, which would allow us to recover all the emission with a spectral $\alpha \geq -0.8$[2], typically associated with the non-thermal plasma located at a few kpc from the stellar disk (Ignesti et al., 2023). The proposed SKA multi-band study, which can also probe the recent star formation rate on different time-scales (Condon, 1992; Kennicutt and Evans, 2012), could be further combined with studies of star formation history in the optical spectrum, which provide the star formation quenching time-scale, and with HI imaging, which measures the ISM fraction removed from the galaxy to address the open question of the effectiveness and speed of quenching from RPS in dense environment.

The SKA, thanks to the unprecedented combination of resolution and sensitivity, will also permit us to explore larger cosmological volumes than is currently possible. To assess its potential in detecting RPS tails at increasing cosmological distances, in Figure 3 (bottom panel), we show the observable fraction of a typical RPS tail located as a function of the redshift that would be recovered in 1 hr observation by SKA. Here we propose a simplified framework in which we use the semi-empirical radio tail profile presented in Ignesti et al. (2023) to simulate two extreme possibilities, a small tail with a starting luminosity, which is the luminosity at the stellar disk, of 10^{26} erg s^{-1} Hz^{-1} and a stripping velocity of 400 km s^{-1}, and an extreme case with an initial luminosity of 10^{28} erg s^{-1} Hz^{-1} and stripping velocity of 800 km s^{-1}. For simplicity, we assume the magnetic field for which the radiative losses are minimized $B \simeq 1.9 \cdot (1+z)^2$ μG and we neglect the potential role of projection effects on the observed tail projected length. The flux density profile predicted by the model is then converted into a surface brightness profile under the simplified assumption that the tail width is always resolved, and hence that the only significant dimension affected by the cosmological distance is the tail projected length. The resulting surface brightness profiles at increasing redshift z are then compared with the expected sensitivity and resolution that will be achieved by SKA in AA4 configuration to determine which is the largest angular distance at which the radio tail can be considered as marginally resolved, which we define as the maximum angular distance at which the emission can be detected with a signal-to-noise ratio higher than three and for which the corresponding angular size, not counting for the stellar disk, is larger than the angular resolution. For reference, we include in this exercise also the sensitivity and resolution currently achieved by the LOFAR Two-metre Sky Survey (LoTSS, Shimwell et al., 2017), which provided us the LoTSS Jellyfish Galaxies sample (Roberts et al., 2021a,b). It emerges that LOFAR has been formidable in detecting radio tails up to $z \simeq 0.05$, but the limited resolution and sensitivity makes ti difficult to resolve radio tails, and hence locate RPS candidates, beyond $z = 0.1$. We note, however, that deep LOFAR pointings (Botteon et al., 2022) have managed to detect RPS tails up to $z = 0.08$ (Ignesti et al., 2023). In the AA4 configuration, SKA-Low will permit us to recover, at least, 50% of the radio tail lengths up to $z \simeq 0.1$, thus expanding the cosmological volume previously

[1] https://sensitivity-calculator.skao.int/

[2] The synchrotron spectral index is defined as $S(\nu) \propto \nu^{\alpha}$, where $S(\nu)$ is the flux density observed at the frequency ν and α is the spectral index.

probed by LOFAR by a factor ~ 9, with the advantage of observing a different part of the sky as discussed above. For reference, by considering the 4955 clusters at $z < 0.1$ with mass higher than 5×10^{13} $M_{\odot}$, which contain a total of 67759 member galaxies (Wen and Han, 2024), based on the typical number of RPS candidates per cluster ($\sim 9\%$, Vulcani et al., 2023), we can expect to detect hundreds of new candidates, effectively improving the current statistic by more than an order of magnitude. SKA-Mid, albeit suffering from the intrinsic observed tail decrease resulting from the higher observed frequency, thanks to the higher angular resolution and sensitivity, will be able to resolve the RPS radio tails up to $z \simeq 0.5$. The increased cosmological volume that will be probed by SKA will further expand the RPS galaxy statistics in clusters and groups, and will potentially help us to study RPS in more rare, extreme environments such as the most massive galaxy clusters or the Cosmic Web filaments. These future high-redshift radio-selected samples will be an ideal target to be explored with a wide-field, high-angular resolution optical survey, such as the EUCLID mission (Euclid Collaboration et al., 2025) the LSST survey at Vera C. Rubin telescope (Ivezić et al., 2019), and the next-generation Roman Space Telescope (Observations Time Allocation Committee and Community Survey Definition Committees, 2025), or with the future high-angular resolution camera on the ELT (Davies et al., 2010). Future SKA developments, such as the construction of longer baselines for SKA-Low, could further increase the importance of SKA in future studies. Reaching sub-kpc physical resolution would allow us to conduct detailed studies of the resolved nonthermal properties, such as high-resolution spectral index mapping or small-scale Hα-radio continuum comparison to evaluate how the local ISM-ICM properties or the star formation spatial distribution influence the nonthermal ISM properties.

4 Conclusions

The study of star-forming galaxies in clusters and groups permits us to explore both how the environment shapes the evolution of galaxies and how the ISM evolves under extreme conditions, providing us with important insights to interpret the evolution of multi-phase plasmas. At the same time, these studies bridge between clusters and galaxies studies, radio and optical observations, being thus the crossroads of many astrophysical cases. Radio continuum studies have demonstrated to play a key role by opening us a window on the nonthermal ISM and by providing us with large, unbiased samples of RPS candidates. The SKA's crucial contribution will be in the following areas: I) greatly increase the statistics of RPS candidates both by opening the southern sky at low frequencies, thanks to SKA-Low, and by expanding the explored cosmological volume from $z \simeq 0.05$ to $z \simeq 0.5$, thanks to SKA-Mid. The crucial improvement in the sample size, which could be achieved by the end of the AA* phase thanks to opening of the Southern sky at low frequencies with SKA-Low, will permit us to build new samples for follow-up multi-wavelength studies; II) map the extraplanar magnetic fields with kpc-scale resolution, hence exploring the extraplanar magnetic fields elusive properties; III) routinely detect the stripped plasma synchrotron emission down to $\alpha \gtrsim -1$, providing us a deep view on the stripped nonthermal ISM evolution and its role in the context of ICM microphysics studies. These results will be transformative for the field, both in terms of an increase in statistics and in physical details of the stripped ISM evolution. An important feature of these studies is that they will greatly synergize with galaxy cluster and group studies, representing an excellent ancillary case for future observations.

References

J. E. Barnes and L. Hernquist. *Annual Review of Astronomy and Astrophysics*, 30:705–742, Jan. 1992. doi: 10.1146/annurev.aa.30.090192.003421.

R. Beck and M. Krause. *Astronomische Nachrichten*, 326(6):414–427, July 2005. doi: 10.1002/asna.200510366.

A. Biviano et al. *APJ*, 965(2):117, Apr. 2024. doi: 10.3847/1538-4357/ad2c09.

A. Boselli, M. Fossati, and M. Sun. *A&AR*, 30(1):3, Dec. 2022. doi: 10.1007/s00159-022-00140-3.

A. Botteon et al. *Science Advances*, 8(44):eabq7623, 2022. doi: 10.1126/sciadv.abq7623. URL https://www.science.org/doi/abs/10.1126/sciadv.abq7623.

H. Chen et al. *MNRAS*, 496(4):4654–4673, Aug. 2020. doi: 10.1093/mnras/staa1868.

W. Choi et al. *APJ*, 999(1):116, Mar. 2026. doi: 10.3847/1538-4357/ae39ca.

J. J. Condon. *Annual Review of Astronomy and Astrophysics*, 30:575–611, Jan. 1992. doi: 10.1146/annurev.aa.30.090192.003043.

R. Davies et al. In I. S. McLean, S. K. Ramsay, and H. Takami, editors, *Ground-based and Airborne Instrumentation for Astronomy III*, volume 7735 of *Society of Photo-Optical Instrumentation Engineers (SPIE) Conference Series*, page 77352A, July 2010. doi: 10.1117/12.856379.

F. de Gasperin et al. In *Advancing Astrophysics with the SKA – II (AASKAII)*. 2026. arXiv search: Report number AASKAII/deGasperin01.

A. Dressler. *APJ*, 236:351–365, Mar. 1980. doi: 10.1086/157753.

L. J. Dursi and C. Pfrommer. *APJ*, 677:993–1018, 4 2008. doi: 10.1086/529371.

L. J. Dursi and C. Pfrommer. *APJ*, 677(2):993–1018, Apr. 2008. doi: 10.1086/529371.

H. Ebeling, C.-J. Ma, and E. Barrett. *APJs*, 211:21, Apr. 2014. doi: 10.1088/0067-0049/211/2/21.

H. W. Edler et al. *A&A*, 683:A149, Mar. 2024. doi: 10.1051/0004-6361/202348301.

Euclid Collaboration et al. *A&A*, 697:A1, May 2025. doi: 10.1051/0004-6361/202450810.

R. J. Farber, M. Ruszkowski, S. Tonnesen, and F. Holguin. *MNRAS*, 512(4):5927–5941, June 2022. doi: 10.1093/mnras/stac794.

A. Franchetto et al. *APJl*, 922(1):L6, Nov. 2021. doi: 10.3847/2041-8213/ac3664.

M. Fumagalli et al. *MNRAS*, 445:4335–4344, Dec. 2014. doi: 10.1093/mnras/stu2092.

G. Gavazzi and W. Jaffe. *A&A*, 186:L1, Nov. 1987.

M. Girardi et al. *APJ*, 404:38, Feb. 1993. doi: 10.1086/172256.

F. Govoni and L. Feretti. *International Journal of Modern Physics D*, 13:1549–1594, 2004. doi: 10.1142/S0218271804005080.

J. E. Gunn and J. R. G. III. *APJ*, 176:1–+, 8 1972. doi: 10.1086/151605.

A. Ignesti et al. *APJ*, 937(2):58, Oct. 2022a. doi: 10.3847/1538-4357/ac8cf6.

A. Ignesti et al. *APJ*, 924(2):64, Jan. 2022b. doi: 10.3847/1538-4357/ac32ce.

A. Ignesti et al. *A&A*, 675:A118, 7 2023. doi: 10.1051/0004-6361/202346517.

A. Ignesti et al. *A&A*, 675:A118, July 2023. doi: 10.1051/0004-6361/202346517.

A. Ignesti et al. *APJ*, 977(2):219, Dec. 2024. doi: 10.3847/1538-4357/ad919b.

A. Ignesti et al. *A&A*, 708:A65, Mar. 2026. doi: 10.1051/0004-6361/202558622.

Ž. Ivezić et al. *APJ*, 873(2):111, Mar. 2019. doi: 10.3847/1538-4357/ab042c.

Y. L. Jaffé et al. *MNRAS*, 476(4):4753–4764, June 2018. doi: 10.1093/mnras/sty500.

J. D. P. Kenney, J. H. van Gorkom, and B. Vollmer. *AJ*, 127:3361–3374, June 2004. doi: 10.1086/420805.

J. D. P. Kenney et al. *APJ*, 780:119, Jan. 2014. doi: 10.1088/0004-637X/780/2/119.

R. C. Kennicutt and N. J. Evans. *Annual Review of Astronomy and Astrophysics*, 50:531–608, Sept. 2012. doi: 10.1146/annurev-astro-081811-125610.

R. I. Klein, C. F. McKee, and P. Colella. *APJ*, 420:213, 1 1994. doi: 10.1086/173554.

D. V. Lal et al. *APJ*, 934(2):170, Aug. 2022. doi: 10.3847/1538-4357/ac7a9b.

Y. Li et al. *MNRAS*, 521(3):4785–4791, May 2023. doi: 10.1093/mnras/stad874.

F. Loi et al. In *Advancing Astrophysics with the SKA – II (AASKAII)*. 2026. arXiv search: Report number AASKAII/Loi01.

M. S. Longair. *High Energy Astrophysics*. 2011.

A. C. C. Lourenço et al. *MNRAS*, 526(4):4831–4847, Dec. 2023. doi: 10.1093/mnras/stad2972.

M. McCourt, R. M. O'Leary, A.-M. Madigan, and E. Quataert. *MNRAS*, 449(1):2–7, May 2015. doi: 10.1093/mnras/stv355.

C. F. McKee and L. L. Cowie. *APJ*, 215:213–225, July 1977. doi: 10.1086/155350.

B. Moore et al. *Nature*, 379:613–616, Feb. 1996. doi: 10.1038/379613a0.

A. Moretti et al. *APJ*, 889(1):9, Jan. 2020. doi: 10.3847/1538-4357/ab616a.

A. Müller et al. *Nature Astronomy*, 5:159–168, Jan. 2021. doi: 10.1038/s41550-020-01234-7.

E. J. Murphy et al. *APJ*, 694(2):1435–1451, Apr 2009. doi: 10.1088/0004-637X/694/2/1435.

P. E. J. Nulsen. *MNRAS*, 221:377–392, Jul 1986. doi: 10.1093/mnras/221.2.377.

R. Observations Time Allocation Committee and C. Community Survey Definition Committees. *arXiv e-prints*, art. arXiv:2505.10574, May 2025. doi: 10.48550/arXiv.2505.10574.

A. G. Pacholczyk. *Radio astrophysics. Nonthermal processes in galactic and extragalactic sources*. 1970.

G. Peluso et al. *APJ*, 927(1):130, Mar. 2022. doi: 10.3847/1538-4357/ac4225.

C. Pfrommer and L. J. Dursi. *Nature Physics*, 6:520–526, 7 2010. doi: 10.1038/nphys1657.

C. Pfrommer and L. J. Dursi. *Nature Physics*, 6(7):520–526, July 2010. doi: 10.1038/nphys1657.

B. M. Poggianti et al. *AJ*, 151(3):78, Mar. 2016. doi: 10.3847/0004-6256/151/3/78.

B. M. Poggianti et al. *Nature*, 548:304–309, Aug. 2017a. doi: 10.1038/nature23462.

B. M. Poggianti et al. *APJ*, 844:48, July 2017b. doi: 10.3847/1538-4357/aa78ed.

B. M. Poggianti et al. *APJ*, 887(2):155, Dec. 2019. doi: 10.3847/1538-4357/ab5224.

B. M. Poggianti et al. *APJ*, 887:155, 12 2019. doi: 10.3847/1538-4357/ab5224.

M. Ramatsoku et al. In *Advancing Astrophysics with the SKA – II (AASKAII)*. 2026. arXiv search: Report number AASKAII/Ramatsoku01.

J. Rasmussen, T. J. Ponman, and J. S. Mulchaey. *MNRAS*, 370(1):453–467, July 2006. doi: 10.1111/j.1365-2966.2006.10492.x.

T. A. Rintoul et al. *MNRAS*, 543(4):4321–4334, Nov. 2025. doi: 10.1093/mnras/staf1718.

I. D. Roberts and L. C. Parker. *MNRAS*, 495(1):554–569, June 2020. doi: 10.1093/mnras/staa1213.

I. D. Roberts et al. *A&A*, 650:A111, June 2021a. doi: 10.1051/0004-6361/202140784.

I. D. Roberts et al. *A&A*, 652:A153, Aug. 2021b. doi: 10.1051/0004-6361/202141118.

I. D. Roberts et al. *APJ*, 941(1):77, Dec. 2022a. doi: 10.3847/1538-4357/ac9e9f.

I. D. Roberts et al. *A&A*, 658:A44, Feb. 2022b. doi: 10.1051/0004-6361/202142294.

I. D. Roberts et al. *A&A*, 689:A22, Sept. 2024a. doi: 10.1051/0004-6361/202450672.

I. D. Roberts et al. *A&A*, 683:A11, Mar. 2024b. doi: 10.1051/0004-6361/202347977.

E. Rohr et al. *MNRAS*, 524(3):3502–3525, Sept. 2023. doi: 10.1093/mnras/stad2101.

M. Ruszkowski, M. Brüggen, D. Lee, and M. S. Shin. *APJ*, 784(1):75, Mar. 2014. doi: 10.1088/0004-637X/784/1/75.

C. L. Sarazin. *X-ray emission from clusters of galaxies*. 1988.

T. W. Shimwell et al. *A&A*, 598:A104, Feb. 2017. doi: 10.1051/0004-6361/201629313.

T. W. Shimwell et al. *A&A*, 622:A1, Feb 2019. doi: 10.1051/0004-6361/201833559.

T. W. Shimwell et al. *A&A*, Jan. 2022. ISSN 0004-6361, 1432-0746. doi: 10.1051/0004-6361/202142484. URL https://www.aanda.org/10.1051/0004-6361/202142484.

R. Smith et al. *APJ*, 934(1):86, July 2022. doi: 10.3847/1538-4357/ac7ab5.

R. Smith et al. *APJ*, 934:86, 7 2022. doi: 10.3847/1538-4357/ac7ab5.

R. J. Smith et al. *MNRAS*, 408:1417–1432, 11 2010. doi: 10.1111/j.1365-2966.2010.17253.x.

M. Sparre, C. Pfrommer, and K. Ehlert. *MNRAS*, 499:4261–4281, 10 2020. doi: 10.1093/mnras/staa3177.

M. Sparre, C. Pfrommer, and E. Puchwein. *MNRAS*, 527:5829–5842, 1 2024. doi: 10.1093/mnras/stad3607.

M. Sparre, C. Pfrommer, and E. Puchwein. *A&A*, 691:A259, Nov. 2024. doi: 10.1051/0004-6361/202450544.

L. J. Spitzer. *Physical Processes in the Interstellar Medium, 1978*. 1978.

M. Sun et al. *Nature Astronomy*, 6:270–274, Dec. 2021. doi: 10.1038/s41550-021-01516-8.

S. Tonnesen, G. L. Bryan, and J. H. van Gorkom. *APJ*, 671(2):1434–1445, Dec. 2007. doi: 10.1086/523034.

J. H. van Gorkom. In J. S. Mulchaey, A. Dressler, and A. Oemler, editors, *Clusters of Galaxies: Probes of Cosmological Structure and Galaxy Evolution*, page 305, Jan. 2004.

M. P. van Haarlem et al. *A&A*, 556:A2, Aug. 2013. doi: 10.1051/0004-6361/201220873.

T. Venturi et al. *A&A*, 660:A81, Apr. 2022. doi: 10.1051/0004-6361/202142048.

B. Vollmer, V. Cayatte, C. Balkowski, and W. J. Duschl. *APJ*, 561(2):708–726, Nov. 2001. doi: 10.1086/323368.

B. Vollmer, R. Beck, J. D. P. Kenney, and J. H. van Gorkom. *AJ*, 127(6):3375–3381, June 2004. doi: 10.1086/420802.

B. Vollmer et al. *A&A*, 553:A116, May 2013. doi: 10.1051/0004-6361/201321163.

B. Vollmer et al. *A&A*, 692:A4, Dec. 2024. doi: 10.1051/0004-6361/202450435.

B. Vulcani et al. *APJl*, 866(2):L25, Oct. 2018. doi: 10.3847/2041-8213/aae68b.

B. Vulcani et al. *APJ*, 899(2):98, Aug. 2020. doi: 10.3847/1538-4357/aba4ae.

B. Vulcani et al. *APJ*, 927(1):91, Mar. 2022. doi: 10.3847/1538-4357/ac4809.

B. Vulcani et al. *APJ*, 949(2):73, June 2023. doi: 10.3847/1538-4357/acc5e2.

A. B. Watts et al. *Publications of the Astronomical Society of Australia*, 40:e017, Apr. 2023. doi: 10.1017/pasa.2023.14.

Z. L. Wen and J. L. Han. *APJs*, 272(2):39, June 2024. doi: 10.3847/1538-4365/ad409d.